Molecular Dissection of Radixin: Distinct and Interdependent Functions of the Amino- and Carboxy-Terminal Domains

Michael D. Henry, Charo Gonzalez Agosti, and Frank Solomon

Department of Biology and Center for Cancer Research, Massachusetts Institute of Technology, Cambridge, Massachusetts 02139

Abstract. The ERM proteins—ezrin, radixin, and moesin—occur in particular cortical cytoskeletal structures. Several lines of evidence suggest that they interact with both cytoskeletal elements and plasma membrane components. Here we described the properties of full-length and truncated radixin polypeptides expressed in transfected cells. In stable transfectants, exogenous full-length radixin behaves much like endogenous ERM proteins, localizing to the same cortical structures. However, the presence of full-length radixin or its carboxy-terminal domain in cortical structures correlates with greatly diminished staining of endogenous moesin in those structures, suggesting that radixin and moesin compete for a limiting factor required for normal associations in the cell. The results also reveal distinct roles for the amino- and carboxy-terminal domains. At low levels relative to endogenous radixin, the carboxy-terminal polypeptide is associated with most of the correct cortical targets except cleavage furrows. In contrast, the amino-terminal polypeptide is diffusely localized throughout the cell. Low level expression of full-length radixin or either of the truncated polypeptides has no detectable effect on cell physiology. However, high level expression of the carboxy-terminal domain dramatically disrupts normal cytoskeletal structures and functions. At these high levels, the amino-terminal polypeptide does localize to cortical structures, but does not affect the cells. We conclude that the behavior of radixin in cells depends upon activities contributed by separate domains of the protein, but also requires modulating interactions between those domains.

MANY experiments demonstrate that the cytoskeleton influences the topography, behavior, and organization of the plasma membrane. However, the detailed molecular basis for this regulation is not clearly understood. A crucial part of solving this problem is the identification of proteins that mediate interactions between components of the plasma membrane and the cytoskeletal polymers. The highly related ezrin, radixin, and moesin proteins—the ERM[1] proteins—are good candidates for molecules that play such a role. Each of these proteins was first isolated from distinct tissues (Bretscher, 1983; Tsukita et al., 1989; Lankes et al., 1988). Antisera against these proteins show that they occur in cellular domains marked by a close juxaposition of the plasma membrane and underlying cytoskeleton. Such domains include microvilli in cultured cells and intestinal epithelia (Bretscher, 1983), the marginal band of nucleated erythrocytes (Birgbauer and Solomon, 1989), filopodia and lamellipodia in migrating cells (Birgbauer, 1991), neuronal growth cones (Goslin et al., 1989; Birgbauer et al., 1991), and cleavage furrows in dividing cells (Sato et al., 1991).

Molecular cloning of the genes encoding the ERM proteins (Gould et al., 1989; Funayama et al., 1991; Lankes and Furthmayr, 1991) demonstrated that they share 70% overall amino acid identity and that their amino termini are about 35% identical to the amino terminus of band 4.1 (Conboy et al., 1986). The inclusion of the ERM proteins and related proteins, like merlin, which is thought to be involved in neuro-fibromatosis type II (Trofatter et al., 1993; Rouleau et al., 1993), in the band 4.1 superfamily (Rees et al., 1990) is suggestive since some evidence indicates that band 4.1 links the plasma membrane and underlying cytoskeleton in human erythrocytes (Anderson and Lovrien, 1984) and that its amino-terminal domain may be important for interaction with the integral membrane protein glycophorin (Leto et al., 1986).

In addition to their cortical localization, there is also direct experimental evidence indicating involvement of ERM proteins in plasma membrane–cytoskeleton interactions. First, a drug interference experiment shows that depolymerization of microtubules disrupts the localization of ERM proteins to cortical structures of growth cones (Goslin et al., 1989; Gonzalez Agosti, Ch., unpublished observations). Second, transiently expressed polypeptides representing the amino-

Address all correspondence to Frank Solomon, Department of Biology and Center for Cancer Research, Massachusetts Institute of Technology, Cambridge, MA 02139. Tel.: (617) 253-3026. Fax: (617) 253-6272.

1. *Abbreviations used in this paper*: DAPI, 4,6-diamidino-2-phenylindole; ERM, ezrin, radixin, and moesin; HA, hemagglutinin.

and carboxy-terminal portions of ezrin localize to cell surface microvilli (Algrain et al., 1993). Third, a functional test of ERM proteins suggests a role consistent with such bivalent interactions: diminution of ERM levels by application of antisense oligonucleotides affects both cell–cell and cell–substratum adhesion (Takeuchi et al., 1994). Other studies have identified putative ERM protein binding partners in the plasma membrane and cytoskeleton. All three ERM proteins coimmunoprecipitate with the integral membrane protein CD44 (Tsukita et al., 1994) in several cell types, and the carboxyl-terminal domain of ezrin interacts with F-actin, but not G-actin in vitro (Turunen et al., 1994).

Although this evidence is consistent with ERM proteins acting as molecular links between the cytoskeleton and plasma membrane, the purposes these links serve, how they are established and maintained, and whether ERM proteins are involved in processes other than physically linking these two organelles are outstanding questions. Their presence in both dynamic structures such as the protrusive lamellipodia and comparatively stable structures such as the marginal band suggests that the interactions between ERM proteins and cortical binding partners are under tight spatial and temporal control. For instance, Bretscher (1989) noted that ezrin was rapidly phosphorylated and recruited to membrane ruffles in epidermal growth factor–stimulated A431 cells, but the mechanisms that regulate this sort of ERM protein behavior are still unknown.

It has been suggested that different ERM proteins might occupy structurally or functionally distinct subcellular domains (Sato et al., 1992). However, other studies, including the present one, indicate that ERM proteins localize to identical subcellular domains (Franck et al., 1993; Winckler et al., 1994). That such highly similar proteins occupy the same subcellular locales raises the possibility that these proteins may have at least partially overlapping functions. Indeed, in the antisense inhibition experiment mentioned, the cell adhesion phenotypes are manifest only when levels of all three ERM proteins are reduced in concert; although there is also some evidence in this study that the roles for the ERM proteins may not be entirely similar (Takeuchi et al., 1994).

With these issues in mind, we describe an analysis of exogenously expressed radixin polypeptides in cultured cells. The results demonstrate that exogenous radixin can behave like endogenous ERM proteins, localizing to the same cortical structures. We also show evidence suggesting that radixin and moesin share an important common binding partner and that these proteins may be functionally interchangeable. These properties of the full-length radixin molecule are mimicked by low levels of the carboxy-terminal domain of the protein, but not the amino-terminal domain. At higher levels, the carboxy-terminal domain in the absence of the amino-terminal domain profoundly alters cell morphology and division–phenotypes that may reflect functions for ERM proteins. Our results demonstrate the activities associated with distinct domains of radixin as well as crucial interactions between those domains.

Materials and Methods

Cell Culture

NIH-3T3 cells were maintained in DME supplemented with 10% bovine calf serum (HyClone, Logan, UT). HtTA-1 cells (a HeLa cell line derivative stably expressing the tetracycline-repressible transactivating element [Gossen and Bujard, 1992]) were obtained with permission from Dr. Hermann Bujard (University of Heidelberg; Heidelberg, FRG) from the laboratory of Dr. Hans-Martin Jack (Loyola University; Chicago, IL). Isolation and characterization of HtTA-1 cells has been described by Damke et al. (1995). HtTA-1 cells were maintained in DME supplemented with 10% FBS (HyClone) and 400 μg/ml G-418 sulfate (Geneticin; GIBCO BRL, Gaithersburg, MD). All cells were incubated at 37°C under 5% CO_2 in a humidified chamber and routinely subcultured.

DNA Constructs and Transfection

We introduced the influenza hemagglutinin (HA) epitope tag (YPYDVPDYA; Field et al., 1988) onto the amino and carboxyl termini of both full-length and truncated forms of the murine radixin coding sequence in the following manner. First, we synthesized two double-stranded oligonucleotides containing the following features in a 5′ to 3′ orientation and in the same translational reading frame: oligonucleotide 1 comprises an initiation codon (which is part of a 5′ NcoI site in both oligonucleotides 1 and 2), followed by the nucleic acid sequence encoding the HA epitope, the 6-base XhoI cloning site, and finally, a stop codon; oligonucleotide 2 comprises an initiation codon, followed by the 6-base XhoI cloning site, the nucleic acid sequence encoding the HA epitope, and finally, a stop codon. Also, to maintain the proper reading frame in these oligonucleotide sequences with respect to the initiation codon, a codon for alanine was inserted at what becomes residue 2 in the translated protein. All oligonucleotides used in this study were synthesized in the MIT Biopolymers Facility (Cambridge, MA). Using T4 DNA ligase, we inserted each of these oligonucleotides into the NcoI/BamHI-digested pMFG retroviral vector (Dranoff et al., 1993) obtained from Dr. Richard Mulligan (MIT). The resulting plasmids were named pMFG-HAN (derived from oligonucleotide 1) and pMFG-HAC (derived from oligonucleotide 2). All enzymes used for recombinant DNA work were obtained from New England Biolabs Inc. (Beverly, MA) and were used according to the manufacturer's specifications. Next, we prepared murine radixin coding sequences for insertion into pMFG-HAN and pMFG-HAC by PCR-mediated amplification (GeneAmp PCR Kit; Perkin-Elmer Corp., Branchburg, NJ), with a Perkin-Elmer DNA thermal cycler, from the pR2ESS plasmid containing a cDNA clone of murine radixin (obtained from Dr. Akira Nagafuchi; National Institute for Physiological Sciences; Okazaki, Japan [Funayama et al., 1991]). The following oligonucleotide primer pairs were used to direct the synthesis of full-length and truncated forms of radixin while simultaneously adding XhoI cloning sites in frame with and directly apposed to the 5′ and 3′ ends of the radixin coding sequence: full length (residues 2–583), primer 1–5′-CCGCTCGAGCCGAAGCCAATCAATGTAAG and primer 2–5′-CCGCTCGAGCATGGCTTCCAACTCATCG; amino terminus (residues 2–318), primers 1 and 3–5′-CCGCTCGAGCTGCTTCTGATGCAAAACC; carboxyl terminus (residues 319–583), primer 2 and 4–5′-CGGCTCGAGCTAGAAAGGGCACAATTAG. After treatment with T4 polynucleotide kinase, the resulting PCR products were ligated into the EcoRI site of pUC19 made blunt by treatment with Klenow enzyme and dephosphorylated by treatment with calf intestinal phosphatase. The resulting plasmids, pUC-RAD (full length), pUC-RADN (amino terminus), and pUC-RADC (carboxyl terminus), were cut with XhoI, and the radixin inserts were separated from the pUC vector on an agarose gel and purified with a Qiaex gel extraction kit (Qiagen, Chatsworth, CA). These three radixin fragments with XhoI sites on their 5′ and 3′ ends were inserted into the unique XhoI site adjoining the HA epitope sequence in pMFG-HAN and pMFG-HAC, and those ligants containing inserts in the proper orientation were identified by diagnostic restriction enzyme digests. Note, owing to the extra sequence added by the XhoI site, insertion of the radixin fragments into pMFG-HAN and pMFG-HAC resulted in the addition of a leucine and a glutamate residue immediately flanking both the amino and carboxyl termini of the radixin coding sequence. The resulting six plasmids, representing the full-length and amino- and carboxy-terminal portions of murine radixin bearing the HA epitope tag at either their amino or carboxyl termini, were designated pMFG-HAN-RAD, pMFG-HAN-RADN, pMFG-HAN-RADC, pMFG-HAC-RAD, pMFG-HAC-RADN, and pMFG-HAC-RADC (the names of these plasmids correspond to the constructs shown in Fig. 2 *A*). The integrity of the junctions between the radixin coding sequence and the flanking sequence containing the HA epitope was confirmed by DNA sequencing (Sequenase Version 2.0 DNA Sequencing Kit; United States Biochemical Corp., Cleveland, OH).

For expression of the HA–radixin constructs in HtTA-1 cells, we digested pMFG-HAN-RAD, pMFG-HAN-RADN, pMFG-HAN-RADC, pMFG-HAC-RAD, pMFG-HAC-RADN, and pMFG-HAC-RADC separately with NcoI, treated the linearized plasmids with Klenow enzyme to blunt the NcoI ends, digested with BamHI, and isolated those fragments containing the

radixin coding sequence plus the HA epitope tag by purification from an agarose gel. These fragments were ligated into the multiple cloning site of the tetracycline-regulatable expression plasmid pUHD 10-3 (kindly provided by Dr. Hermann Bujard), which we prepared by digestion with EcoRI, treatment of the linearized plasmid with Klenow enzyme to blunt the EcoRI ends, digestion with BamHI, and purification on an agarose gel. Insertion of HA-radixin constructs into pUHD 10-3 was confirmed by diagnostic restriction enzyme digests. The resulting plasmids were named pUHD-HAN-RAD, pUHD-HAN-RADN, pUHD-HAN-RADC, pUHD-HAC-RAD, pUHD-HAC-RADN, and pUHD-HAC-RADC. The polypeptides encoded by these plasmids are identical to those expressed from the pMFG-derived plasmids.

Both stable and transient transfection protocols were modifications of the calcium phosphate transfection protocol of Graham and van der Eb (1973). Plasmid DNAs were prepared from Qiagen columns. For stable transfection of NIH-3T3 cells, pMFG-HAN-RAD, pMFG-HAN-RADN, pMFG-HAN-RADC, pMFG-HAC-RAD, pMFG-HAC-RADN, and pMFG-HAC-RADC were cotransfected with pSV2-neo (Southern and Berg, 1982) at a 10:1 molar ratio, respectively. Stably transfected NIH-3T3 cells were selected in the presence of 600 μg/ml G-418 sulfate. The resultant colonies were picked, expanded in the continuous presence of the selecting agent, and stored in liquid nitrogen. Cell lines derived in this manner were periodically passaged through medium containing 600 μg/ml G-418 sulfate. HtTA-1 cells were transfected as described by Damke et al. (1995).

Antibodies

Polyclonal antibodies 464, 457, and 454 raised against unique peptides from murine ezrin, radixin, and moesin, respectively, have been described previously (Winckler et al., 1994). They were affinity purified as described by Winckler et al. (1994) except that anti-radixin antibody 457 was affinity eluted from the radixin-immunoreactive band of chicken erythrocytes. mAb 12CA5 (Niman et al., 1983) was obtained from Berkeley Antibody Co. (Richmond, CA).

Protein Extracts and Immunoblotting

We prepared whole-cell extracts from cultured cells by first lysing the subconfluent monolayers in PBS containing 2% SDS and a protease inhibitor cocktail consisting of 0.04 U/ml aprotinin, 1 μg/ml PMSF, 1 μg/ml leupeptin, and 1 μg/ml pepstatin (Sigma Chemical Co., St. Louis, MO). An aliquot of this lysate was reserved for determination of protein concentration by the method of Lowry et al. (1951) using a detergent-compatible analysis system from Bio Rad Laboratories (Melville, NY). To the remaining lysate, we added Laemmli sample buffer (Laemmli, 1970) and boiled this mixture for 5 min.

For immunoblotting, we separated protein samples on a 7.5% polyacrylamide gel with a 5% stacker according to the method of Laemmli (1970). Proteins were electrophoretically transferred to 0.2-μm nitrocellulose filters (Schleicher & Schuell, Inc., Keene, NH) essentially as described by Tobin et al. (1979). Transfer of protein to filter and equivalency of loads were confirmed by staining with 0.2% Ponceau S (Sigma Chemical Co.) in 3% TCA. For blotting with antibodies 464, 457, and 454, the nitrocellulose filters were first blocked with 5% BSA (Sigma Chemical Co.) in TBS supplemented with 0.1% Tween-20 and 0.05% sodium azide for 2 h. Next, the affinity-purified antibodies were diluted 1:100 into blocking buffer and incubated overnight at room temperature, washed extensively in TBS supplemented with 0.1% Tween-20, incubated for 1 h in blocking buffer containing a 1:1,000 dilution of ^{125}I-labeled protein A (DuPont NEN, Boston, MA), and washed in TBS supplemented with 0.1% Tween-20 again. For blotting with mAb 12CA5, the nitrocellulose filters were first blocked with 5% nonfat dry milk (Nestle Food Co., Glendale, CA) in TBS supplemented with 0.1% Tween-20 and 0.05% sodium azide overnight. Next, mAb 12CA5 was diluted 1:1,000 into blocking buffer and incubated for 1 h at room temperature, washed extensively in TBS supplemented with 0.1% Tween-20, incubated for 1 h in blocking buffer containing a 1:10,000 dilution of horseradish peroxidase-conjugated sheep anti-mouse IgG F(ab')$_2$ (Amersham Corp., Arlington Heights, IL), and washed in TBS supplemented with 0.1% Tween-20 again. ^{125}I signal was detected autoradiographically on DuPont-NEN Reflection Film at −70°C using a DuPont Reflection intensifying screen and quantified using a PhosphorImager (Molecular Dynamics, Inc., Sunnyvale, CA). Horseradish peroxidase signal was detected by enhanced chemiluminescence with the Lumiglo reagent kit (Kirkegaard and Perry Laboratories, Gaithersburg, MD) on DuPont- NEN Reflection Film at room temperature.

Indirect Immunofluorescence Microscopy

Cells grown on glass coverslips were fixed for 30 min in PBS containing 4% paraformaldehyde, permeabilized for 10 min in PBS containing 0.5% NP-40, and washed three times in PBS. For immunostaining, fixed, permeabilized cells were first blocked in PBS containing 10% normal goat serum (Vector Laboratories, Inc., Burlingame, CA). The cells were then incubated with the appropriate primary antibody diluted in PBS containing 1% BSA for 30 min at 37°C, washed three times in PBS, incubated with the appropriate secondary antibody—FITC-conjugated goat anti-rabbit IgG F(ab')$_2$ (Tago, Burlingame, CA) for antibodies 464, 457, and 464 and rhodamine- or FITC-conjugated goat anti-mouse IgG F(ab')$_2$ (Organon Teknika, Durham, NC) for mAb 12CA5—diluted in PBS containing 1% BSA for 30 min at 37°C, and washed three times in PBS. In some experiments, during secondary antibody incubation, cells were stained with rhodamine-conjugated phalloidin (Molecular Probes Inc., Eugene, OR) and/or 4,6-diamidino-2-phenylindole (DAPI; Sigma Chemical Co.) to reveal F-actin and DNA, respectively. The coverslips were mounted onto glass slides using Gelvatol mounting medium containing the anti-fade agent 1,4-diazabicyclo[2,2,2] octane at 15 mg/ml (Aldrich Chemical Co., Milwaukee, WI).

Cells were examined by conventional microscopy on an Axioplan microscope (Carl Zeiss Inc., Thornwood, NY) using 63× 1.4 N.A. and 100× 1.3 N.A. objectives. Images were recorded on Tri-X-Pan 400 film (Eastman Kodak Co., Rochester, NY). For confocal microscopy, cells were examined with an MRC 600 scanning laser confocal microscope (Bio Rad Laboratories). FITC-labeled second antibody and rhodamine-labeled phalloidin were detected with a yellow high sensitivity filter and blue high sensitivity filter, respectively. Images taken from a video monitor were recorded on Plus-X-Pan 125 film (Eastman Kodak Co.).

Results

Expression and Localization of ERM Proteins in NIH-3T3 Cells

We previously showed that NIH-3T3 cells express each of the ERM proteins (Winckler et al., 1994). Antisera generated against unique peptides from the predicted sequence of ezrin (antibody 464), radixin (antibody 457), and moesin (antibody 454) each recognized a distinct band in extracts of NIH-3T3 cells. By immunofluorescence, the antibodies against radixin and moesin brightly stained cortical structures such as microvilli and filopodia as well as the cleavage furrows of dividing cells (Fig. 1, *B–H*). The antibodies also stained lamellipodia and ruffling edges, although less intensely (data not shown). These localizations are consistent with those reported in other cell types (Bretscher, 1983; Franck et al., 1993; Sato et al., 1992). Anti-ezrin antiserum did not give detectable staining in these cells (Fig. 1 *A*). This result may represent different localization or lower levels of ezrin, but it is not a property of the anti-ezrin antiserum, which gives definitive staining in another cell type (Winckler et al., 1994). Thus, NIH-3T3 cells express each of the ERM proteins, and two of them—radixin and moesin— localize in patterns indistinguishable from one another.

Stable Expression of Epitope-tagged Forms of Radixin in NIH-3T3 Cell Lines

We generated constructs encoding the full-length protein and its amino- and carboxy-terminal portions, fused to the HA epitope. The division into amino- and carboxy-terminal polypeptides occurs at codon 318, so the amino-terminal polypeptide contains all of the sequence homologous to band 4.1. The inclusion of the epitope tag allowed us to distinguish immunologically the exogenous from the endogenous gene products. Versions of the constructs bearing the HA epitope sequence at either their amino or carboxyl terminus (see

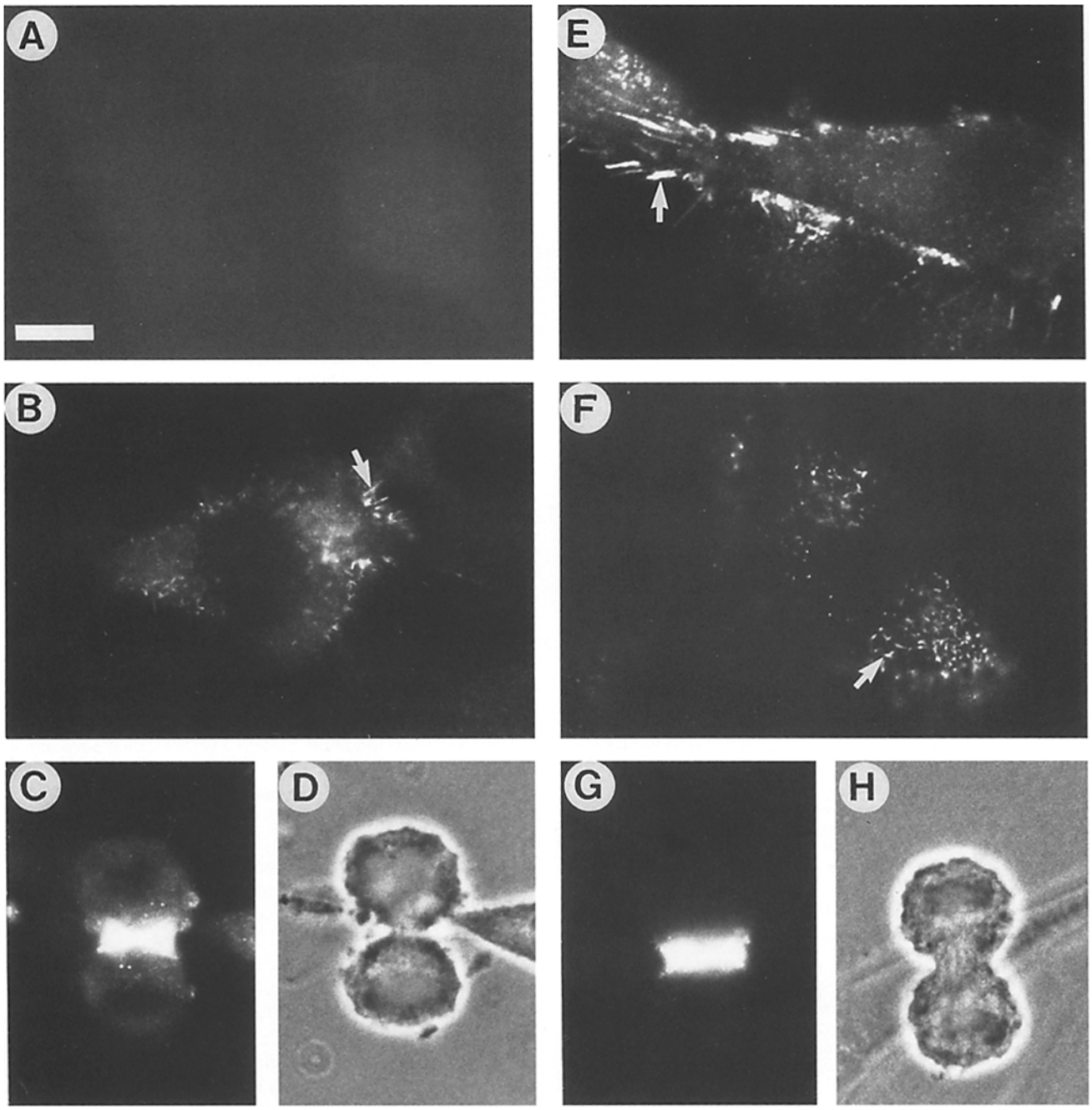

Figure 1. Localization of endogenous ERM proteins in NIH-3T3 cells. NIH-3T3 cells were processed for indirect immunofluorescence with anti-ezrin antibody 464 (*A*), anti-radixin antibody 457 (*B–D*), and anti-moesin antibody 454 (*E–H*) as described in Materials and Methods. Anti-radixin and anti-moesin specifically label cortical structures such as filopodia (*arrows* in *B* and *E*), microvilli (*arrow* in *F*), and cleavage furrows (*C* and *G*). Phase contrast images of dividing cells in *C* and *G* are shown in *D* and *H*, respectively. Anti-ezrin is not detectable in any discrete structure (*A*). Bar, 20 μm.

Materials and Methods) allowed us to control for effects of the extra sequence on the conformation or function of the proteins. Fig. 2 *A* shows a schematic diagram of the constructs.

To generate stable NIH-3T3 lines expressing these proteins, we cotransfected the pMFG retroviral vector, containing each of the radixin constructs, and pSV2-neo and selected for resistance to G-418 sulfate (see Materials and Methods). We recovered tens to hundreds of drug-resistant colonies for each of the constructs in each of two independent transfections. We picked 5–10 drug-resistant colonies for each construct from each transfection, expanded, and screened for expression of HA–radixin constructs by immunoblotting with mAb 12CA5. As expected, the expression levels varied somewhat among lines derived from each of the constructs—as much as 10-fold—as assessed by Western blots. Fig. 2 *B* shows such blots on extracts from lines expressing relatively high levels of each of the six HA–radixin

constructs. The apparent sizes of both the full-length and the truncated epitope-tagged constructs were as expected considering the addition of the HA sequence. Previous reports documented the anomalously high apparent molecular mass of both full-length ezrin (Gould et al., 1989) and the carboxy-terminal domain of ezrin (Algrain et al., 1993) on SDS-PAGE compared with that calculated from the predicted amino acid sequence. Like ezrin, the apparent molecular masses of the HA-tagged forms of both the full-length and the carboxy-terminal polypeptides of radixin are higher (81 and 46 kD, respectively) than their calculated molecular masses (69 and 35 kD, respectively).

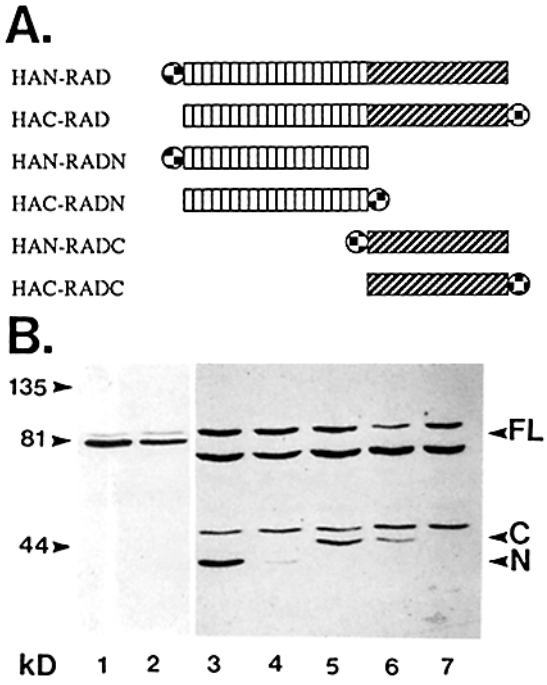

Figure 2. Stable expression of HA–radixin constructs in NIH-3T3 cells. (*A*) Diagram of HA–radixin constructs. We added the influenze HA epitope ( ) to the amino (*HAN*) and carboxyl (*HAC*) termini of the coding sequence of full-length murine radixin, amino acids 1–583 (*RAD*); the amino terminus ( ), amino acids 1–318 corresponding to the band 4.1 homology (*RADN*); and the carboxyl terminus ( ), amino acids 319–583 containing the putative F-actin binding domain (*RADC*), as described in Materials and Methods. (*B*) Western blot analysis of lysates taken from stably transfected NIH-3T3 cell lines. 20 μg of total protein taken from lines stably expressing HA–radixin constructs was analyzed by immunoblotting with mAb 12CA5 directed to the HA epitope as described in Materials and Methods. Lane *1*, HAC-RAD; lane *2*, HAN-RAD; lane *3*, HAN-RADN; lane *4*, HAC-RADN; lane *5*, HAN-RADC; lane *6*, HAC-RADC; lane *7*, untransfected NIH-3T3. The film used for lanes *3–7* was exposed 20-fold longer than the film for lanes *1* and *2*. Positions of the full-length (*FL*), amino-terminal (*N*), and carboxy-terminal (*C*) polypeptides are indicated to the right of the blot. Several species dependent on mAb 12CA5, but unrelated to the HA–radixin polypeptides, appeared at the longer exposure time used for lanes *3–7*. These species are also detectable in lysates from untransfected NIH-3T3 cells (lane *7*). Despite this background immunoreactivity detected by Western blotting, immunostaining untransfected NIH-3T3 cells with mAb 12CA5 gave a low background and no discrete structures were stained (see Fig. 3 *H*). Positions of molecular weight standards are indicated to the left of the blot.

The levels of expression of the two full-length constructs—HAC-RAD and HAN-RAD, tagged at their carboxy- and amino-termini, respectively (Fig. 2 *B*, lanes *1* and *2*)—are comparable to one another. In contrast, the levels of the truncated constructs were significantly lower than those of the full-length constructs; for comparison, the region of the autoradiograph depicted in Fig. 2 *B*, lanes *3–7*, was exposed 20 times longer than were lanes *1* and *2*. At these longer exposures, bands recognized by mAb 12CA5 but not dependent upon transfection become apparent (Fig. 2 *B*, lane *7*). Since the epitope-tagged full-length radixin protein specified by the transfected sequence migrates slightly more slowly in SDS-PAGE than does the endogenous radixin molecule, we could compare their relative steady-state levels in these stable lines by blotting with antibody 457 and measuring the signal by PhosphorImager. By this assay, the steady-state level of the full-length tagged proteins was approximately fourfold higher than that of endogenous radixin (data not shown). Because expression levels of the truncated HA–radixin constructs were much lower (>20-fold) than those of the full-length HA–radixin constructs, we estimate that the expression levels of the truncated HA–radixin polypeptides are at least fivefold lower than the level of endogenous radixin.

In general, the cells expressing HA–radixin constructs were indistinguishable from the parental line with respect to cell morphology and growth rate (see Figs. 3 and 4). The one exception is that cultures expressing the carboxy-terminal polypeptides contained multinucleated cells at a relatively high frequency. The frequency did vary, however, among the individual lines and in any case occurred more robustly in cells expressing high levels of the carboxy-terminal constructs (see below).

Subcellular Localization of HA–Radixin Polypeptides in NIH-3T3 Cell Lines

We examined the localization of each of the six HA–radixin polypeptides by immunofluorescence microscopy. The HAC-RAD protein (the full-length molecule tagged on its carboxyl terminus) was in the same cellular domains as endogenous radixin shown in Fig. 1: in cortical structures such as cell surface microvilli, filopodia, and cleavage furrows and, less intensely, in ruffling edges and lamellipodia (Fig. 3, *A–D*). However, the same full-length radixin polypeptide with the epitope tag at its amino terminus (HAN-RAD) displayed no distinct localization and instead was present diffusely in the cytoplasm (Fig. 3, *E–G*). In particular, the HAN-RAD protein was not concentrated at the cell cortex. Neither of the amino-terminal polypeptides, HAN-RADN and HAC-RADN, localized to discrete structures and, like HAN-RAD, appeared to be diffuse throughout the cytoplasm (Fig. 4, *A–C*). Both of the carboxy-terminal polypeptides, HAN-RADC and HAC-RADC, showed localization patterns that were similar, but not identical, to that of HAC-RAD. Like the full-length protein, the carboxy-terminal polypeptides were present in cortical structures. Although, compared with either HAC-RAD or endogenous radixin, they were more enriched in ruffling edges and lamellipodia (Fig. 4 *F*). In two ways, however, the localization of the carboxy-terminal polypeptides differed strikingly from that of HAC-RAD. First, in some cells, these polypeptides coaligned with linear, phalloidin-positive structures near the ventral surface

of the cell (Fig. 4, *G* and *H*, *large arrows*) that likely represent stress fibers. This result is consistent with the localization of the carboxy-terminal polypeptide of ezrin in transient transfection experiments (Algrain et al., 1993). Second, we could not detect HAN-RADC or HAC-RADC in cleavage furrows (compare Fig. 4, *D* and *E*, with Fig. 3, *C* and *D*).

These localization characteristics described for each polypeptide were the same in all independently isolated lines examined. We also stably expressed these constructs in a different cell line, P19 embryonal carcinoma cells, and in these cells the localization properties of the polypeptides were the same as in NIH-3T3 cells (Henry, M., and N. Torres, unpublished observations).

Displacement of Endogenous Moesin by Epitope-tagged Radixin Polypeptides

Taking advantage of the fact that the endogenous moesin and the products of the transfected genes were distinguishable by

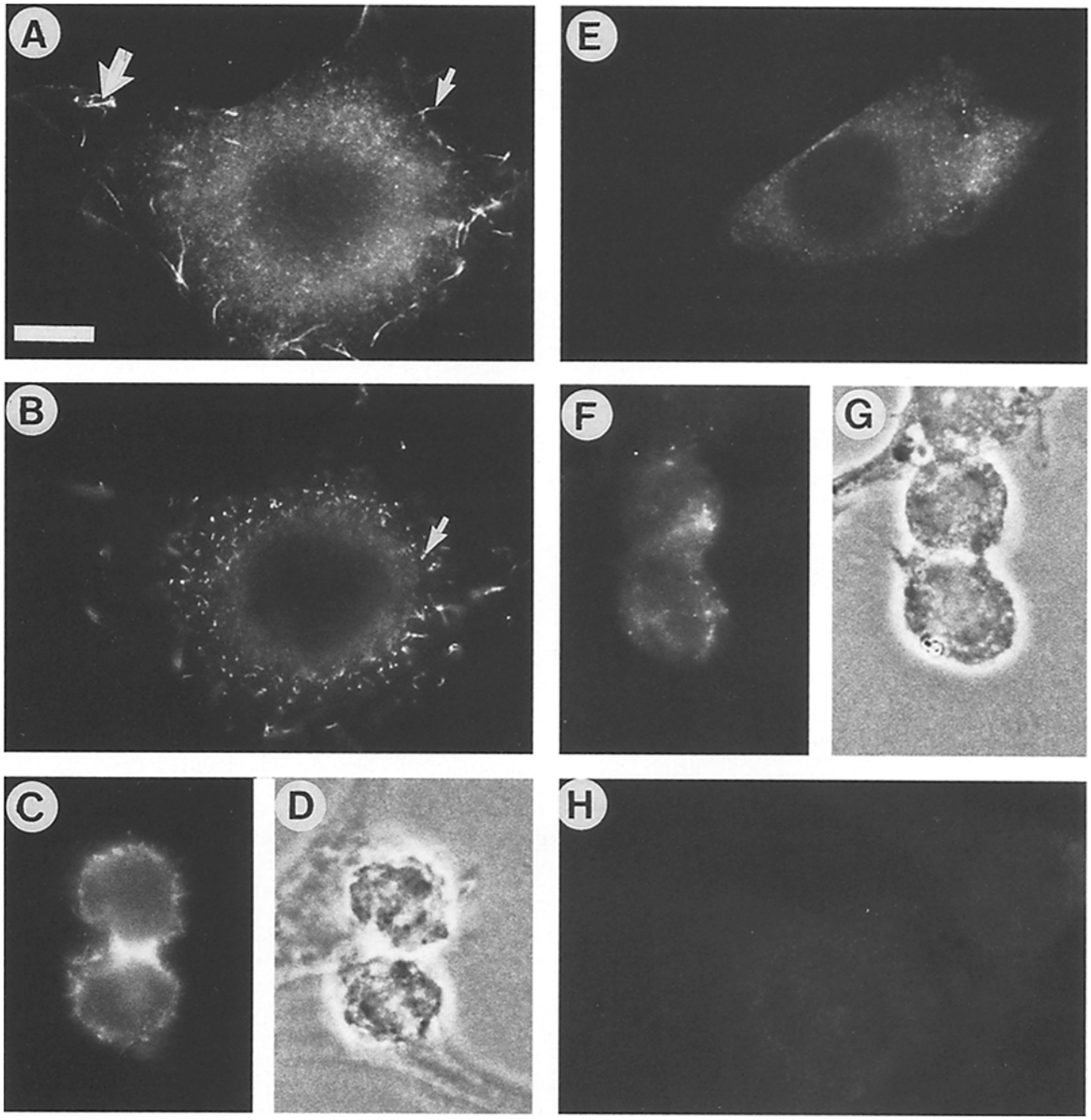

Figure 3. Localization of full-length HA–radixin polypeptides in NIH-3T3 cell lines. NIH-3T3 cell lines stably expressing HAC-RAD (*A–D*) or HAN-RAD (*E–G*) and untransfected NIH-3T3 cells (*H*) were processed for indirect immunofluorescence with mAb 12CA5 as indicated in Materials and Methods. *A* and *B* are, respectively, ventral and dorsal focal planes of the same cell. HAC-RAD is localized to cortical structures including filopodia (*small arrow* in *A*), ruffling edges (*large arrow* in *A*), microvilli (*arrow* in *B*), and cleavage furrows (*C*). HAN-RAD does not localize to discrete structures in either nondividing (*E*) or dividing (*F*) cells. *D* and *G* are phase contrast images of dividing cells shown in *C* and *F*. No specific staining is detectable in untransfected cells (*H*). Bar, 20 μm.

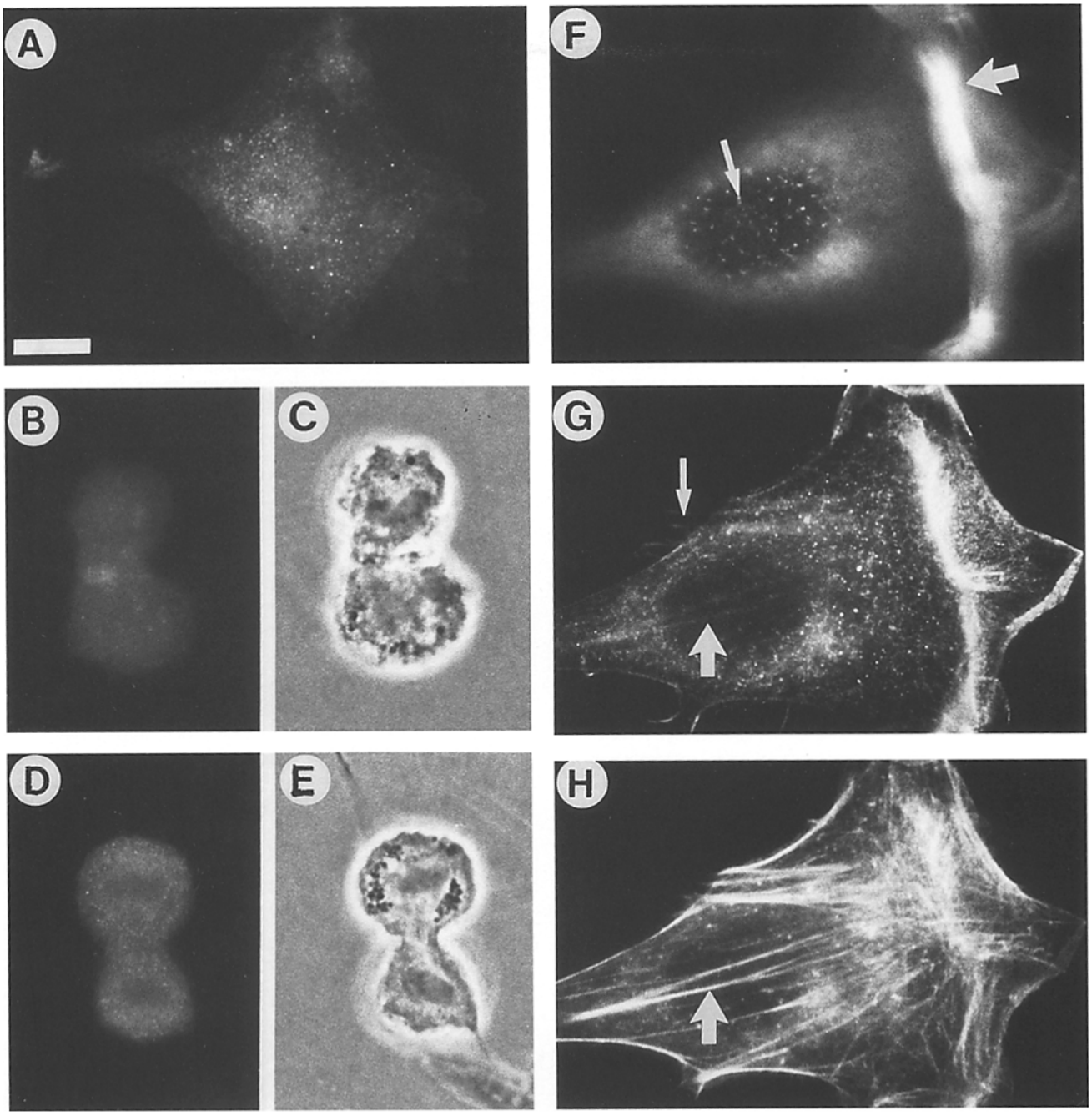

Figure 4. Localization of truncated HA–radixin polypeptides in NIH-3T3 cell lines. NIH-3T3 cell lines stably expressing HAN-RADN (*A–C*) or HAC-RADC (*D–H*) were processed for indirect immunofluorescence with mAb 12CA5 and phalloidin as indicated in Materials and Methods. HAN-RADN does not localize to discrete structures in either nondividing (*A*) or dividing (*B*) cells. *F* and *G* are, respectively, dorsal and ventral focal planes of the same cell. Results similar to those shown for HAN-RADN were obtained for lines expressing HAC-RADN (data not shown). HAC-RADC is localized to cortical structures including microvilli (*small arrow* in *F*), ruffling edges (*large arrow* in *F*), and filopodia (*small arrow* in *G*). Staining in ruffling edges is much more intense in lines expressing carboxy-terminal constructs. HAC-RADC also associates with linear elements in the ventral cytoplasm (*large arrow* in *G*) that coalign with F-actin–containing microfilaments revealed by phalloidin staining (*large arrow* in *H*). HAC-RADC does not localize to cleavage furrows in dividing cells (*D*). *H* is the rhodamine channel showing phalloidin staining in the same focal plane as *G*. *C* and *E* are the phase contrast images of the dividing cells shown in *B* and *D*. Results similar to those shown for HAC-RADC were obtained for lines expressing HAN-RADC (data not shown). Bar, 20 μm.

their reactivity with different antibodies, we performed double label immunofluorescence on the stably transfected cell lines. The results demonstrate that those radixin polypeptides that did localize affect the behavior of endogenous moesin. As shown in Fig. 5, cells expressing HAC-RAD and HAC-RADC, both of which showed typical ERM localization, exhibited a substantial diminution of anti-moesin staining in microvilli and filopodia (Fig. 5, *A*, *B*, *G*, and *H*). A

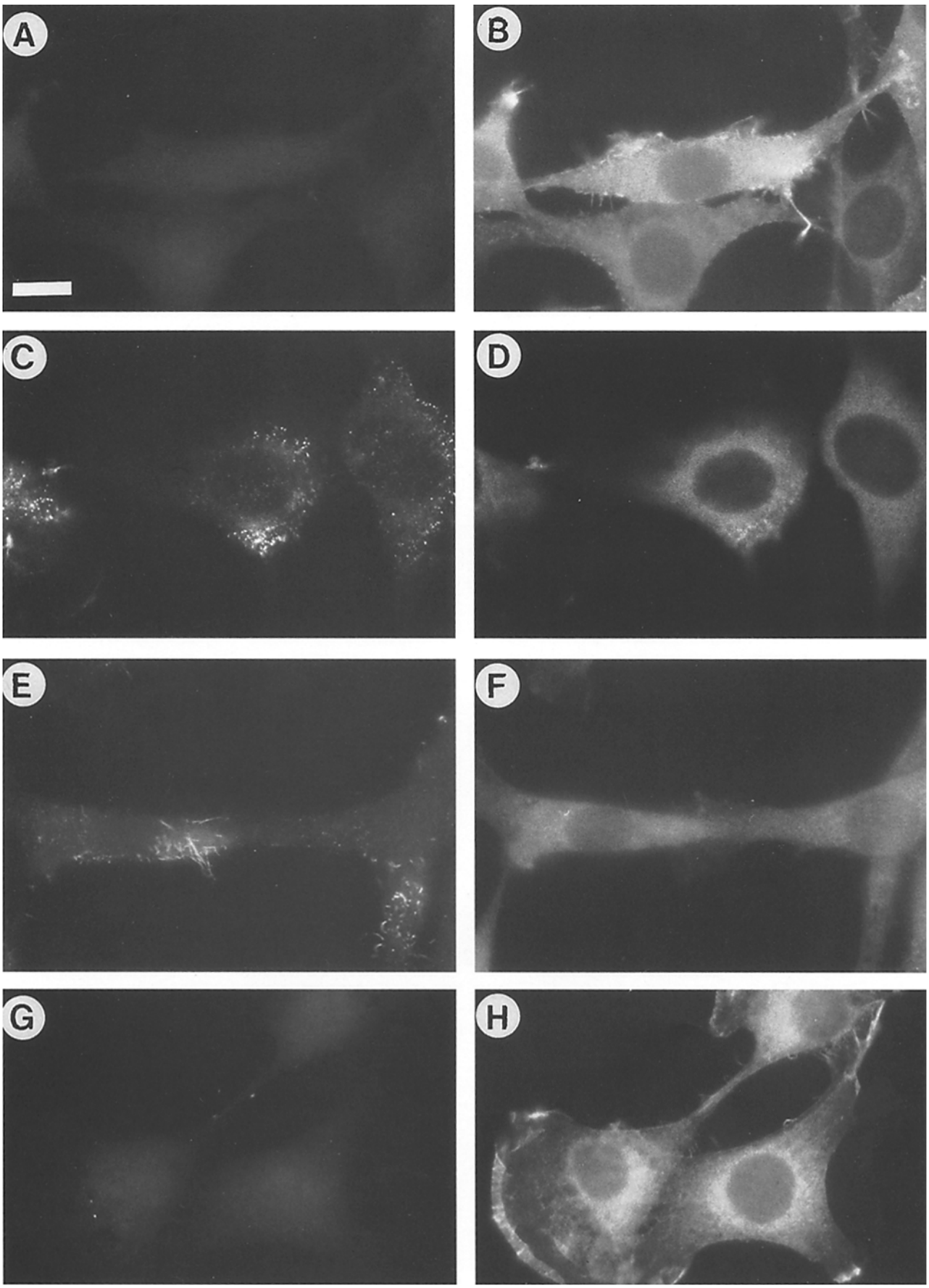

Figure 5. Displacement of endogenous moesin from cortical structures by HA–radixin polypeptides in NIH-3T3 cells. Lines expressing HA–radixin constructs were processed for indirect immunofluorescence double labeled with anti-moesin antibody 454 (*A*, *C*, *E*, and *G*) and anti-HA mAb 12CA5 (B, D, F, and H). Anti-moesin staining is dramatically reduced in cortical structures in cells expressing HAC-RAD (*A* and *B*) and HAC-RADC (*G* and *H*). Moesin localization in cortical structures was normal in cells expressing HAN-RAD (*C* and *D*) and HAN-RADN (*E* and *F*). Bar, 30 μm.

similar but less dramatic reduction was observed in cells expressing HAN-RADC (data not shown). Moesin localization in HAN-RAD, HAN-RADN, and HAC-RADN lines was quantitatively indistinguishable from that in untransfected cells (Fig. 5, *C–F*). In addition, moesin localization in cleavage furrows was also diminished in cells expressing the full-length polypeptide HAC-RAD. However, cells expressing HAN-RADC or HAC-RADC, which themselves did not localize to cleavage furrows, showed normal moesin staining in that structure (data not shown).

These apparent qualitative differences among the different transfected constructs were not due to a quantitative difference in moesin levels in those lines. Western blotting with antibody 454 demonstrated that all lines expressing HA–radixin constructs maintained similar amounts of moesin and showed no evidence of its down-regulation (data not shown).

Consequences of Transient Expression of HA–Radixin Constructs in HeLa Cells

Some of the results we reported for the amino- and carboxy-terminal domains of radixin in stably transfected NIH-3T3 cells differ from those reported for the corresponding domains of ezrin in transiently transfected CV-1 cells (Algrain et al., 1993). These differences might arise from differences in expression levels of the radixin and ezrin polypeptides in the two experiments. We noted that there were some indications that stable expression of high levels of amino- and/or carboxy-terminal polypeptides might not be tolerated by the cells. First, the highest expression level of each of these polypeptides in stable lines was significantly less than 20% that of the full-length proteins. Second, as has been noted, we detected an abnormally high incidence of multinucleated cells in HAN-RADC and HAC-RADC cultures. For these reasons, we examined the effects of high level, transient expression of full-length and truncated forms of radixin.

We placed the various HA–radixin constructs under the control of the tetracycline-repressible promoter developed by H. Bujard and co-workers (Gossen and Bujard, 1992) and transfected them into HtTA-1 cells, a HeLa cell line derivative stably expressing the essential tetracycline-sensitive transactivator element (see Materials and Methods). HtTA-1 cells, like NIH-3T3 cells, expressed all three ERM proteins. Only radixin and moesin were detected in cortical structures in nondividing cells, but all three proteins were detectable in cleavage furrows (data not shown).

We evaluated the expression of the exogenous genes 48 h after transfection. Western blot analysis showed that the HA–radixin constructs were expressed at approximately equal levels (Fig. 6). This result suggests that the lower steady-state expression levels of the truncated HA–radixin constructs, relative to the full-length versions, that we observed in stably transfected NIH-3T3 cells are not due to inherent instability of the truncated polypeptides. The transient expression level of HA–radixin constructs was ~20-fold higher than the level of endogenous radixin in HtTA-1 cells, as assessed by Western blotting and PhosphorImager analysis of extracts from transfected cultures with antibody 457 (data not shown). Because only 10–40% of cells in these transiently transfected cultures expressed the HA–radixin constructs, the relative expression levels in these cells must be even higher.

By immunofluorescence, HAC-RAD localized to cortical structures, as did endogenous radixin (Fig. 7, *A–C*). HAN-RAD was diffuse in the cytoplasm, even in brightly staining cells (Fig. 7, *D–F*). Thus, the results in transiently transfected HtTA cells expressing these full-length constructs are consistent with those obtained from the stable transfectants of NIH-3T3 cells expressing much lower levels of the full-length constructs. However, in contrast to the results in the stable transfectants, both amino-terminal polypeptides (HAN-RADN and HAC-RADN) were concentrated in cortical structures (Fig. 7, *G–I*). Transient, high level expression of either the full-length or amino-terminal HA–radixin constructs did not result in any gross morphological alterations. There were, however, striking consequences of expressing either of the carboxy-terminal polypeptides at high levels. Many cells exhibited multiple long, tapered processes covering the dorsal surface of the cells that were clearly distinguishable by phase contrast microscopy. Other extensions that made contact with the substratum, like filopodia, were much larger than similar structures in normal cells (Fig. 7, *J–L*). The confocal micrographs shown in Fig. 8 better illustrate the three-dimensional nature of these processes. The processes stained intensely with both mAb 12CA5 and phalloidin, suggesting that they contain F-actin (Fig. 8, *A–F, left* in each). On the contrary, microtubules were not enriched in these processes, and we only occasionally observed them in the wide bases of the processes proximal to the cell soma. In fact, the microtubule arrays in cells expressing HAN-RADC and HAC-RADC appeared similar to that in cells expressing other HA–radixin constructs and in nonexpressing cells (data not shown). In the same population, cells exhibiting weaker immunoreactivity with mAb 12CA5 showed either modest versions of the processes or none at all. We never observed these processes in mAb 12CA5–negative cells or in cells expressing the full-length or amino-terminal HA–radixin constructs.

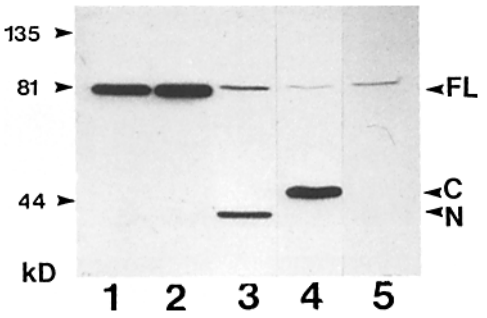

Figure 6. Transient expression of HA–radixin constructs in HtTA-1 cells. Lysates were harvested from HtTA-1 cells 48 h after transfection with HA–radixin constructs. At this time, 10–40% of the cells expressed mAb 12CA5 immunoreactivity as judged by indirect immunofluorescence microscopy. 20 μg of total protein was examined by Western blot analysis with mAb 12CA5. Lane *1*, HAN-RAD; lane *2*, HAC-RAD; lane *3*, HAN-RADN; lane *4*, HAN-RADC; lane *5*, untransfected HtTA-1 cells. Positions of the full-length (*FL*), amino-terminal (*N*), and carboxy-terminal (*C*) polypeptides are indicated to the right of the blot. The species migrating just above the full-length protein is unrelated to expression of HA–radixin constructs and is present in untransfected HtTA-1 cells (lane *5*). Positions of molecular mass standards are indicated to the left of the blot.

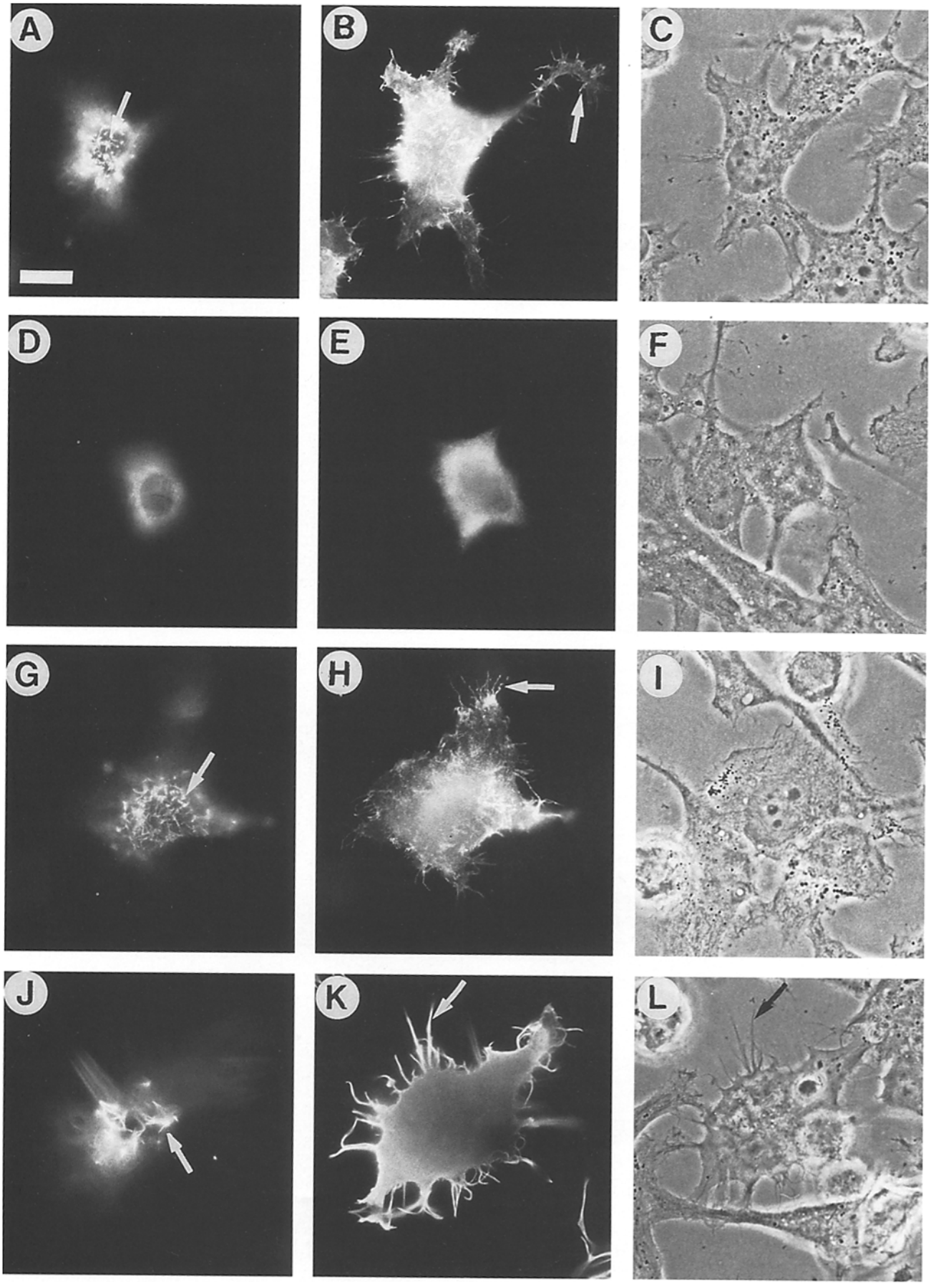
A
B
C
D
E
F
G
H
I
J
K
L

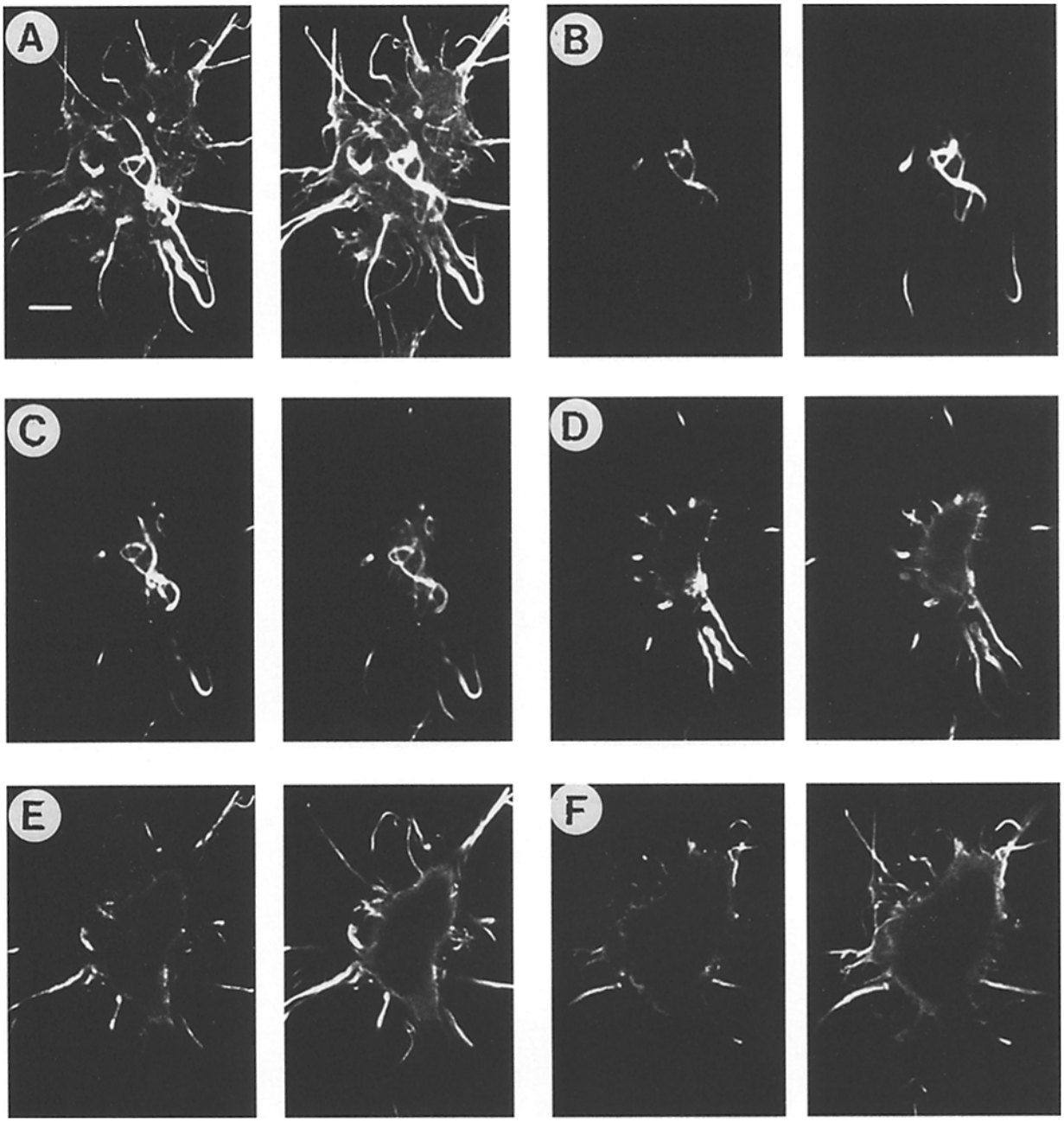

Figure 8. Optical sectioning of HtTA-1 cells transiently expressing HAN-RADC. HtTA-1 cells expressing HAN-RADC were fixed 48 h after transfection and processed for indirect immunofluorescence by double labeling with mAb 12CA5 and phalloidin. Cells were examined by confocal microscopy as described in Materials and Methods. Each panel *A–F* shows the phalloidin channel on the left side and mAb 12CA5 channel on the right side. *A* is a compilation of all focal planes taken in the z dimension. *B–F* are single focal planes taken in 1 μm steps in a dorsal to ventral direction. Processes emanating from the entire dorsal surface of the cell are long, tapered, and filled with F-actin. Bar, 10 μm.

Figure 7. Localization of HA–radixin polypeptides in transiently transfected HtTA-1 cells. HtTA-1 cells transfected with HAC-RAD (*A–C*), HAN-RAD (*D–F*), HAN-RADN (*G– I*), and HAC-RADC (*J–L*) were fixed 48 h after transfection and examined by indirect immunofluorescence microscopy with mAb 12CA5 as described in Materials and Methods. mAb 12CA5 immunoreactivity is shown for the same cell in dorsal (*A*, *D*, *G*, and *J*) and ventral (*B*, *E*, *H*, and *K*) focal planes and in phase contrast (*C*, *F*, *I*, and *L*). HAC-RAD localizes to microvilli (*arrow* in *A*) and to filopodia (*arrow* in *B*). HAN-RAD does not localize to discrete structures (*D* and *E*). HAN-RADN localizes to dorsal microvilli (*arrow* in *G*) and to filopodia in contact with the substratum (*arrow* in *H*). Results similar to those shown for cells transfected with HAN-RADN were obtained for cells transfected with HAC-RADN (data not shown). Expression of HAC-RADC induces the presence of long, tapered processes that can be seen in dorsal focal planes (*arrow* in *J*) and in contact with the substratum (*arrow* in *K*). These processes are clearly visible by phase contrast microscopy (*arrow* in *L*). Results similar to those shown for cells transfected with HAC-RADC were obtained for cells transfected with HAN-RADC (see Fig. 10). Bar, 30 μm.

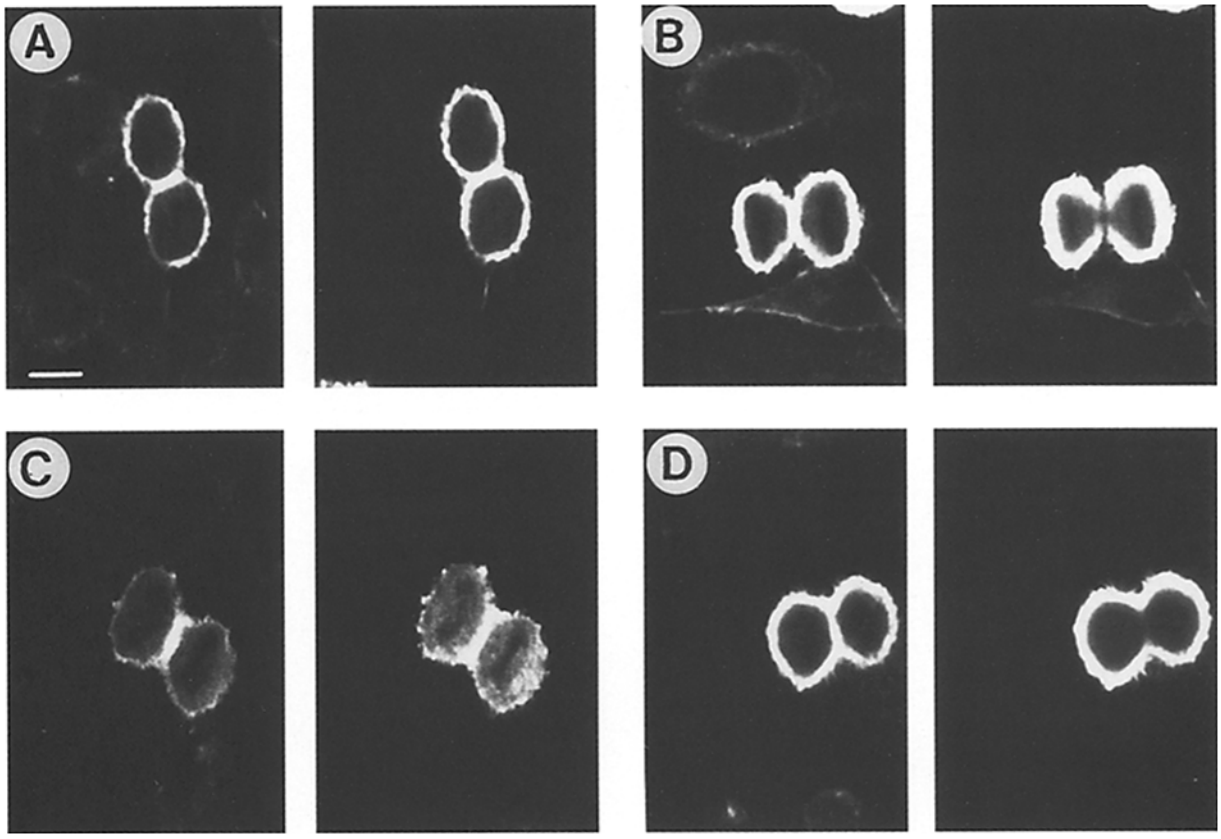

Figure 9. Localization of HA-radixin polypeptides in cleavage furrows of transiently transfected HtTA-1 cells. HtTA-1 cells expressing HA-radixin constructs were fixed 48 h after transfection and processed for indirect immunofluorescence by double labeling with mAb 12CA5 and phalloidin. Cells were examined by confocal microscopy as described in Materials and Methods. Each panel *A–D* shows the phalloidin channel on the left side and mAb 12CA5 channel on the right side. HAC-RAD (*A*) and HAN-RADN (*C*) localize to the F-actin–containing contractile ring, but HAN-RAD (*B*) and HAN-RADC (*D*) do not. Bar, 10 μm.

Because mAb 12CA5 signal intensity made the imaging of cleavage furrows and ventral focal planes by conventional microscopy difficult, we took optical sections with a confocal microscope to examine HA-radixin localization in these areas. Fig. 9 shows cleavage furrows in dividing cells expressing HA-radixin constructs stained with mAB 12CA5 and phalloidin. These images demonstrate that the HAC-RAD polypeptide colocalizes with F-actin throughout the contractile ring, but that HAN-RAD cannot be detected in this structure. However, unlike the situation in the NIH-3T3 cell lines, both of the amino-terminal HA-radixin constructs localized to cleavage furrows in the transiently transfected HtTA-1 cells (HAN-RADN is shown in Fig. 9 *C*). This difference is considered in the Discussion section. However, HAN-RADC, although it colocalized with F-actin in other regions of the cortex, was detectable in the contractile ring (Fig. 9 *D*); HAC-RAD-C showed similar behavior (data not shown). Thus, in HtTA-1 cells expressing high levels of HA-radixin constructs, both the full-length molecule and the amino-terminal domain are capable of localizing to the F-actin–rich cleavage furrow, whereas the same high levels of the carboxy-terminal polypeptides were not detectable in this structure.

Unlike their behavior when stably expressed in NIH-3T3 cells, the transiently expressed amino-terminal polypeptides localized to cortical structures and the carboxy-terminal polypeptides induced the presence of abnormal cortical structures in HtTA-1 cells. We think it likely that these differences between the stable and transient transfection experiments are the result of quantitative differences in expression level and do not arise from differences between NIH-3T3 and HtTA-1 cells. When we transiently transfected NIH-3T3 cells with HAN-RADC and HAC-RADC under the control of a strong β-actin promoter, we also found in the brightly mAb 12CA5–staining cells morphological abnormalities resembling those found in HtTA-1 cells transiently transfected with these constructs, including long, tapered processes. NIH-3T3 cells transiently expressing the full-length and amino-terminal constructs did not show such morphological abnormalities (data not shown).

At the higher levels of expression facilitated by the transient transfection system, none of the HA–radixin constructs, particularly the carboxy-terminal polypeptides, colocalized precisely with ventral F-actin filaments (Fig. 10, *A* and *B*). Instead, expression of the carboxy-terminal polypeptides often disrupted normal phalloidin staining in the ventral cytoplasm. Fig. 11 *C* shows a cell expressing HAN-RADC, stained with both anti-HA antibody and phalloidin. The latter staining was diffuse or punctate, in contrast with the linear elements present in control cells (compare left-hand portions in Fig. 10, *A* and *C*).

Expression of the carboxy-terminal polypeptides appar-

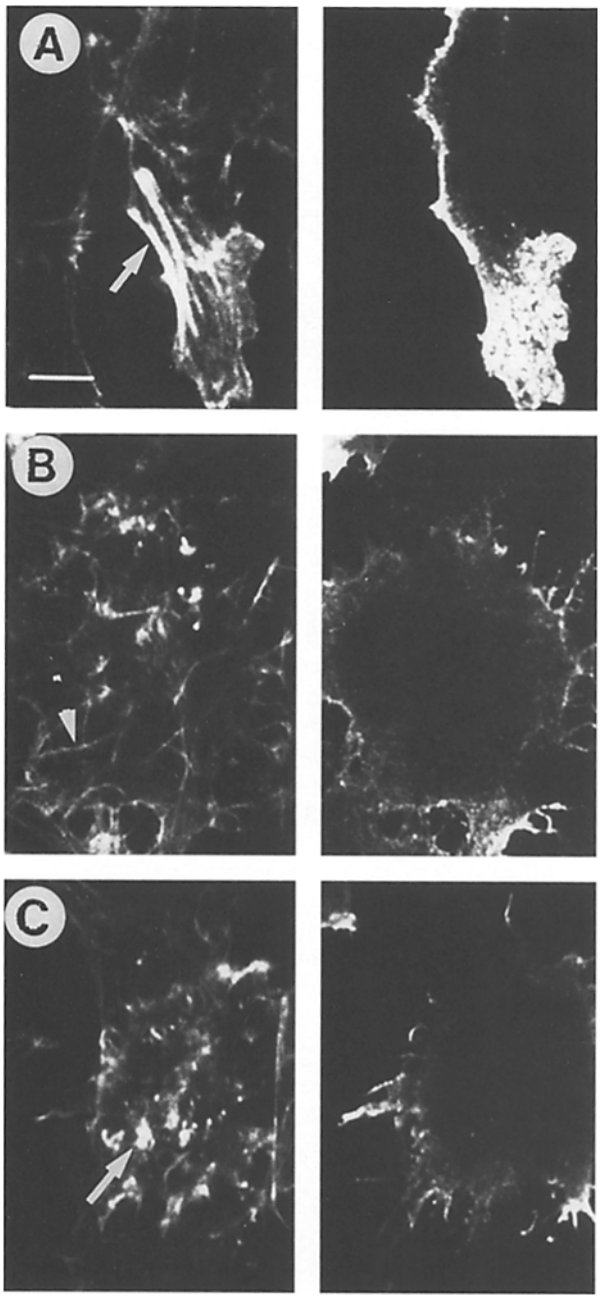

Figure 10. HAN-RADC does not associate with ventral cytoplasmic microfilaments, and its expression can lead to disruption of these structures. HtTA-1 cells expressing HAC-RAD (*A*) and HAN-RADC (*B* and *C*) were fixed 48 h after transfection and processed for indirect immunofluorescence by double labeling with mAb 12CA5 and phalloidin. Cells were examined by confocal microscopy as described in Materials and Methods. Each panel *A–C* shows the phalloidin channel on the left side and the mAb 12CA5 channel on the right side. Cytoplasmic microfilaments were evident in ventral focal planes of cells expressing HAC-RAD (*arrow* in left side of *A*) and in some cells expressing HAN-RADC (*arrow* in left side of *B*), but neither of these HA-radixin constructs colocalized with these structures (compare left and right panels in *A* and *B*). In other cells expressing HAN-RADC (*C*), these linear F-actin structures were disrupted, and phalloidin staining in this region of the cell was diffuse or punctate (*arrow* in left panel of *C*). Bar, 10 μm.

ently also interfered with normal cytokinesis. Many cells brightly staining with mAb 12CA5 had two or more nuclei 48 h after transfection (Fig. 11, *A–C*). We scored the number of nuclei per cell in cultures transfected with each of the six HA-radixin constructs costained with mAb 12CA5 and DAPI. The results showed that the incidence of multinucleated cells is much higher in cells expressing the carboxy-terminal polypeptides than in cells expressing either the full-length or the amino-terminal polypeptides (Fig. 11 *D*). This result was also confirmed by flow cytometry (data not shown).

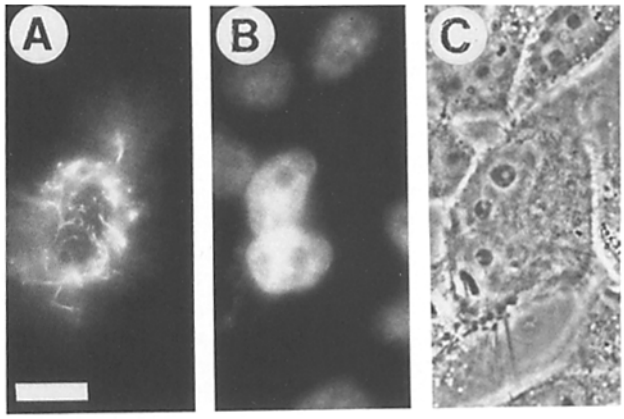

D. PER CENT CELLS WITH TWO (FOUR) NUCLEI

EXPRESSED CONSTRUCT	12CA5(+)	12CA5(-)
HAC-RAD	<1	<1
HAN-RAD	2	0
N-TERMINUS	1	2
C-TERMINUS	24 (5)	<1

Figure 11. Expression of the carboxy-terminal HA-radixin constructs results in an increased number of multinucleated cells. HtTA-1 cells expressing HA-radixin constructs were fixed 48 h after transfection and processed for indirect immunofluorescence by double labeling with mAb 12CA5 and DAPI. A cell expressing HAN-RADC is shown in *A–C*. This mAb 12CA5-positive cell (*A*) has two nuclei that can be seen by DAPI staining (*B*) and by phase contrast (*C*). Cultures of HtTA-1 cells transfected with each of the HA-radixin constructs were scored for mAb 12CA5 immunoreactivity and nuclei number (*D*). 200–400 well-spread, nondividing cells were counted for each construct. The results shown are pooled from three independent transfections. There is a dramatic increase in cultures expressing carboxy-terminal HA-radixin constructs compared with nonexpressing cells in the same culture and with cells expressing either the full-length or the amino-terminal HA-radixin constructs. Bar, 30 μm.

Discussion

NIH-3T3 cells express each of the ERM proteins, and two of them—radixin and moesin—show a typical localization to cortical cytoskeletal structures. To identify the elements of ERM sequence that specify cellular interactions, we expressed full-length radixin and its amino- and carboxy-terminal domains in cultured cells, at both low and high levels relative to endogenous radixin. At low levels, the full-length protein localized to the appropriate cortical structures: ruffling edges, filopodia, and lamellipodia, microvilli, and the cleavage furrow of dividing cells. The carboxy-terminal polypeptide behaved similarly, with two notable exceptions: it did not localize to cleavage furrows, and it localized abnormally, albeit weakly, to some stress fibers. In cells expressing either the full-length or carboxy-terminal polypeptides, the staining of endogenous moesin was substantially diminished. In contrast, the amino-terminal domain of radixin was only diffuse throughout the cell, and its expression had no effect on moesin staining. Only when expressed at levels significantly higher than the endogenous pool did the amino-terminal polypeptide show cortical localization. At those levels, the carboxyl domain induced significant disruptions of normal cytoskeletal structures and functions. These results demonstrate that determinants of radixin localization reside in both the amino- and carboxy-terminal domains of the protein and that these domains may interact in *cis* to achieve localization. The results also suggest that all ERM proteins may have a common intracellular ligand that is both essential and limiting for localization.

Functional Interactions between the Amino- and Carboxy-Terminal Domains of Radixin

Our results suggest that the cellular associations of radixin are not the simple sum of the activities of the parts of the molecule. A previous study found that both the amino- and the carboxy-terminal domains of ezrin associated with cell surface microvilli, but suggested that correct targeting of that protein depends primarily on the amino-terminal sequence (Algrain et al., 1993). The discrepancy between that conclusion and those in this paper may be explained by the effects of high level expression in transient systems versus more modest levels in the stable transfectants examined here. Both amino- and carboxy-terminal domains of radixin do contain determinants of localization, but those determinants apparently can interact with one another in *cis* to account for the properties of the full-length molecule. For example, the carboxy-terminal polypeptide, unlike the full-length molecule, fails to localize to cleavage furrows, binds to stress fibers, and at high levels, disrupts normal cytoskeletal structures and functions. All of these activities are modified in the context of the full-length molecule—that is, when the amino-terminal domain is present in *cis*. Perhaps, then, the amino terminus of radixin exerts a regulatory influence over the activities of the carboxyl terminus. Such as interaction might explain why extensive efforts to detect a direct interaction between F-actin and ezrin in vitro were negative (Bretscher, 1983), whereas the isolated carboxy-terminal polypeptide can bind (Turunen et al., 1994). In cells, too, the carboxy-terminal polypeptide colocalizes with microfilaments (Algrain et al., 1993; and Fig. 9). There is precedent for such intramolecular regulation between domains of a cytoskeletal protein. Johnson and Craig (1994, 1995) demonstrated in vitro that such an interaction modulates the binding of talin to the amino-terminal domain of vinculin and of F-actin to the carboxy-terminal domain.

Interactions of Radixin with Cellular Factors Necessary for Localization

Stable expression of the carboxy-terminal tagged full-length radixin molecule largely abolishes moesin staining. The simplest interpretation of this result is that radixin and moesin compete for some common binding partner that is limiting for localization to cortical structures. This interacting element may be present at the cortex itself; candidate molecules include CD44, which is known to interact with ERM proteins (Tsukita et al., 1994). Alternatively, it could be a cytoplasmic protein with which ERM proteins interact before localization. For example, ERM proteins might localize as homo- or heterooligomeric complexes (Gary and Bretscher, 1993; Andreoli et al., 1994). Overexpression of radixin could compete with other ERM proteins for participation in such complexes.

The carboxy-terminal domain of radixin localizes to cortical structures and, even at levels less than 20% those of endogenous radixin, substantially diminishes moesin staining in cortical structures. This behavior, too, can be explained by competition for a common and necessary binding partner, but also requires that the relative stoichiometry of that partner compared with total ERM proteins is quite small. In addition, either the affinity of the carboxy-terminal polypeptide for the partner is considerably greater than that of full-length ERM proteins—again, suggestive of intramolecular regulation of the interactions of isolated domains—or the pool of endogenous ERM proteins competent to interact with the partner is only a small fraction of the total complement.

Interchangeability of ERM Proteins in NIH-3T3 Cells?

The displacement of moesin by exogenously expressed radixin occurs without any apparent phenotype. This indicates that the tagged version of radixin can substitute for endogenous moesin without seriously disrupting cellular functions such as spreading or cytokinesis. That two ERM proteins, which are 75% identical, are interchangeable at cortical localization sites supports the notion that these proteins may be functionally redundant. Takeuchi et al. (1994) report that antisense inhibition of either ezrin or radixin expression can have phenotypes different from inhibition of moesin expression. Such a phenotypic difference can arise from qualitative differences among the three proteins, but functionally interchangeable elements can give different null phenotypes for quantitative reasons as well (Schatz et al., 1986).

Consequences of High Level Expression of the Carboxy-Terminal Domain of Radixin

High level expression of the carboxy-terminal domain has several negative consequences for cells: it induces the formation of long processes all over the surface of the cell—processes unlike normal cortical extensions such as filopodia or microvilli; it disrupts ventral F-actin filaments; and it interferes with cytokinesis even though the polypeptide itself is not found in cleavage furrows. These phenotypes are

not the simple consequence of overexpressing any actin-associated protein. For example, the carboxy-terminal domain of caldesmon, transiently expressed in CHO cells, associates with and stabilizes F-actin, but does not induce cortical processes (Warren et al., 1994). It is possible that the long processes induced by high levels of this radixin domain sequester a substantial fraction of components required to form F-actin and so indirectly affect cytokinesis. Indeed, the phenotype observed here in NIH-3T3 cells may reflect generalizable interactions of ERM carboxyl domains. Overexpression of the carboxy-terminal domain of the *Drosophila melanogaster* moesin homologue in fission yeast produces irregularly shaped and multinucleated cells (Edwards et al., 1994). If the carboxy-termini of ERM proteins are centrally involved in the organization of the cytoskeleton at particular cortical sites, perhaps modulating membrane protrusive activity at those sites, then the overexpression of this domain could lead to the observed morphological phenotypes.

We thank H. Bujard, R. Mulligan, and A. Nagafuchi for generously sharing reagents vital to this study; D. Smith (MIT, Cambridge, MA) for expert assistance with the confocal microscopy; N. Torres (MIT) for experimental contributions; T. Jacks, B. Kennedy, A. Lander, A. McClatchey, and R. Shaw (all of MIT), and members of our laboratory for insightful discussions and helpful comments on the manuscript. M. D. Henry was supported in part by a National Science Foundation predoctoral fellowship. C. G. Agosti was supported in part by a postdoctoral fellowship from the Swiss National Science Foundation. This work was supported by a grant from the National Institutes of Health (CA53395-03) to F. Solomon.

Received for publication 23 December 1994 and in revised form 14 February 1995.

Note Added in Proof: While this manuscript was in press, Martin et al. (*J. Cell Biol.* 128:1081–1093) reported that the amino-terminal domain of ezrin inhibits in *trans* the cell extension activity of the carboxy-terminal domain in moth ovary cells. We do not detect such a *trans*-acting effect of the domains of radixin in cultured mammalian cells.

References

Algrain, M., O. Turunen, A. Vaheri, D. Louvard, and M. Arpin. 1993. Ezrin contains cytoskeleton and membrane binding domains accounting for its proposed role as a membrane-cytoskeletal linker. *J. Cell Biol.* 120:129–139.

Anderson, R. A., and R. E. Lovrien. 1984. Glycophorin is linked by band 4.1 protein to the human erythrocyte membrane skeleton. *Nature (Lond.).* 307:655–658.

Andreoli, C., M. Martin, R. Le Borgne, H. Reggio, and P. Mangeat. 1994. Ezrin has properties to self-associate at the plasma membrane. *J. Cell Sci.* 107:2509–2521.

Birgbauer, E. 1991. Cytoskeletal interactions of ezrin in differentiated cells. Ph.D. thesis. Massachusetts Institute of Technology, Cambridge, MA.

Birgbauer, E., and F. Solomon. 1989. A marginal band-associated protein has properties of both microtubule- and microfilament-associated proteins. *J. Cell Biol.* 109:1609–1620.

Birgbauer, E., J. H. Dinsmore, B. Winckler, A. D. Lander, and F. Solomon. 1991. Association of ezrin isoforms with the neuronal cytoskeleton. *J. Neurosci. Res.* 30:232–241.

Bretscher, A. 1983. Purification of an 80,000-dalton protein that is a component of the isolated microvillus cytoskeleton, and its localization in non-muscle cells. *J. Cell Biol.* 97:425–432.

Bretscher, A. 1989. Rapid phosphorylation and reorganization of ezrin and spectrin accompany morphological changes induced in A-431 cells by epidermal growth factor. *J. Cell Biol.* 108:921–930.

Conboy, J., Y. K. Kan, S. B. Shohet, and N. Mohandas. 1986. Molecular cloning of protein 4.1, a major structural element of the human erythrocyte membrane skeleton. *Proc. Natl. Acad. Sci. USA.* 83:9512–9516.

Damke, H., M. Gossen, S. Freundlieb, H. Bujard, and S. L. Schmid. 1995. Tightly regulated and inducible expression of a dominant interfering dynamin mutant in stably transformed HeLa cells. *Methods Enzymol.* In press.

Dranoff, G., E. Jaffe, A. Lazenby, P. Golumbek, H. Levitsky, K. Brose, V. Jackson, H. Hamada, D. Pardoll, and R. C. Mulligan. 1993. Vaccination with irradiated tumor cells engineered to secrete murine granulocyte-macrophage colony-stimulating factor stimulates potent, specific, and long-lasting anti-tumor immunity. *Proc. Natl. Acad. Sci. USA.* 90:3539–3543.

Edwards, K. A., R. A. Montague, S. Shepard, B. A. Edgar, R. L. Erikson, and D. P. Kiehart. 1994. Identification of Drosophila cytoskeletal proteins by induction of abnormal cell shape in fission yeast. *Proc. Natl. Acad. Sci. USA.* 91:4589–4593.

Field, J., J.-I. Nikawa, D. Broek, B. MacDonald, L. Rodgers, I. A. Wilson, R. A. Lerner, and M. Wigler. 1988. Purification of a RAS-responsive adenylyl cyclase complex from *Saccharomyces cerevisiae* by use of an epitope addition method. *Mol. Cell. Biol.* 8:2159–2165.

Franck, Z., R. Gary, and A. Bretscher. 1993. Moesin, like ezrin, colocalizes with actin in the cortical cytoskeleton in cultured cells, but its expression is more variable. *J. Cell Sci.* 105:219–231.

Funayama, N., A. Nagafuchi, N. Sato, Sa. Tsukita, and Sh. Tsukita. 1991. Radixin is a novel member of the band 4.1 family. *J. Cell Biol.* 115: 1039–1048.

Gary, R., and A. Bretscher. 1993. Heterotypic and homotypic associations between ezrin and moesin, two putative membrane-cytoskeletal linking proteins. *Proc. Natl. Acad. Sci. USA.* 90:10846–10850.

Goslin, K., E. Birgbauer, G. Banker, and F. Solomon. 1989. The role of cytoskeleton in organizing growth cones: a microfilament-associated growth cone component depends upon microtubules for its localization. *J. Cell Biol.* 109:1621–1631.

Gossen, M., and H. Bujard. 1992. Tight control of gene expression in mammalian cells by tetracycline-responsive promoters. *Proc. Natl. Acad. Sci. USA.* 89:5547–5551.

Gould, K. L., A. Bretscher, F. S. Esch, and T. Hunter. 1989. cDNA cloning and sequencing of the protein-tyrosine kinase substrate, ezrin, reveals homology to band 4.1. *EMBO (Eur. Mol. Biol. Org.) J.* 8:4133–4142.

Graham, F. L., and A. J. van der Eb. 1973. A new technique for the assay of infectivity of human adenovirus DNA. *Virology.* 52:456–467.

Johnson, R. P., and S. W. Craig. 1994. An intramolecular association between the head and tail domains of vinculin modulates talin binding. *J. Biol. Chem.* 269:12611–12619.

Johnson, R. P., and S. W. Craig. 1995. F-actin binding site masked by the intramolecular association of vinculin head and tail domains. *Nature (Lond.).* 373:261–264.

Laemmli, U. K. 1970. Cleavage of structural proteins during the assembly of the head of bacteriophage T4. *Nature (Lond.).* 227:680–685.

Lankes, W., A. Greismacher, J. Gruenwald, R. Schwartz-Albeiz, and R. Keller. 1988. A heparin binding protein involved in inhibition of smooth-muscle cell proliferation. *Biochem. J.* 251:831–842.

Lankes, W. T., and H. Furthmayr. 1991. Moesin: a member of the protein 4.1-talin-ezrin family of proteins. *Proc. Natl. Acad. Sci. USA.* 88:8297–8301.

Leto, T. L., I. Correas, T. Tobe, R. A. Anderson, and W. C. Horne. 1986. Structure and function of human erythrocyte cytoskeletal protein 4.1. *In* Membrane Skeletons and Cytoskeletal-Membrane Associations. V. Bennet, C. M. Cohen, S. Lux, and J. Palek, editors. Alan R. Liss, New York. 201–209.

Lowry, O. H., J. Rosebrough, A. S. Farr, and R. J. Randall. 1951. Protein measurement with the folin phenol reagent. *J. Biol. Chem.* 193:265–275.

Niman, H. L., R. A. Houghten, L. W. Walker, R. A. Reisfeld, I. A. Wilson, J. A. Hogle, and R. A. Lerner. 1983. Generation of protein-reactive antibodies by short peptides is an event of high frequency: implications for the structural basis of immune recognition. *Proc. Natl. Acad. Sci. USA.* 80: 4949–4953.

Rees, D. J. G., S. E. Ades, S. J. Singer, and R. O. Hynes. 1990. Sequence and domain structure of talin. *Nature (Lond.).* 347:685–689.

Rouleau, G. A., P. Merel, M. Lutchman, M. Sanson, J. Zucman, C. Marineau, K. Hoang-Xuan, S. Demczuk, C. Desmaze, B. Plougastel, S. M. Pulst, G. Lenoir, E. Bijlsma, R. Fashold, J. Dumanski, P. Jong, D. Parry, R. Eldridge, A. Aurias, O. Delattre, and G. Thomas. 1993. Alteration in a new gene encoding a putative membrane-organizing protein causes neuro-fibromatosis type 2. *Nature (Lond.).* 363:515–521.

Sato, N., S. Yonemura, T. Obinata, Sa. Tsukita, and Sh. Tsukita. 1991. Radixin, a barbed end-capping actin-modulating protein, is concentrated at the cleavage furrow during cytokinesis. *J. Cell Biol.* 113:321–330.

Sato, N., N. Funayama, A. Nagafuchi, S. Yonemura, Sa. Tsukita, and Sh. Tsukita. 1992. A gene family consisting of ezrin, radixin, and moesin. Its specific localization at actin filament/plasma membrane association sites. *J. Cell Sci.* 103:131–143.

Schatz, P. J., F. Solomon, and D. Botstein. 1986. Genetically essential and nonessential alpha-tubulin genes specify functionally interchangeable proteins. *Mol. Cell. Biol.* 6:3722–3733.

Southern, P. J., and P. Berg. 1982. Transformation of mammalian cells to antibiotic resistance with a bacterial gene under control of the SV40 early region promoter. *J. Mol. Appl. Genet.* 1:327–341.

Takeuchi, K., N. Sato, H. Kasahara, N. Funayama, A. Nagafuchi, S. Yonemura, Sa. Tsukita, and Sh. Tsukita. 1994. Perturbation of cell adhesion and microvilli formation by antisense oligonucleotides to ERM family members. *J. Cell Biol.* 125:1371–1384.

Tobin, H., T. Staehelin, and J. Jordon. 1979. Electrophoretic transfer of proteins from polyacrylamide gels to nitrocellulose sheets; procedure and some

applications. *Proc. Natl. Acad. Sci. USA.* 76:4350–4354.

Trofatter, J. A., M. M. MacCollin, J. L. Rutter, J. R. Murrell, M. P. Duyao, D. M. Parry, R. Eldridge, N. Kley, A. G. Menon, K. Pulaski, V. H. Hasse, C. M. Ambrose, D. Munroe, C. Bove, J. L. Haines, R. L. Martuza, M. E. MacDonald, B. R. Seizinger, M. P. Short, A. J. Buckler, and J. F. Gusella. 1993. A novel moesin-, ezrin-, radixin-like gene is a candidate for the neurofibromatosis 2 tumor suppressor. *Cell.* 72:791–800.

Tsukita, Sa., Y. Hieda, and Sh. Tsukita. 1989. A new 82-kD barbed end-capping protein (radixin) localized in the cell-to-cell adherens junction: purification and characterization. *J. Cell Biol.* 108:2369–2382.

Tsukita, Sa. K. Oishi, N. Sato, J. Sagara, A. Kawai, and Sh. Tsukita. 1994. ERM family members as molecular linkers between the cell surface glycoprotein CD44 and actin-based cytoskeletons. *J. Cell Biol.* 126:391–401.

Turunen, O., T. Wahlstrom, and A. Vaheri. 1994. Ezrin has a COOH-terminal actin binding site that is conserved in the ezrin protein family. *J. Cell Biol.* 126:1445–1453.

Warren, K. S., J. L.-C. Lin, D. D. Wamboldt, and J. J.-C. Lin. 1994. Overexpressin of human fibroblast caldesmon fragment containing actin, Ca^{++}/calmodulin-, and tropomyosin-binding domains stabilizes endogenous tropomyosin and microfilaments. *J. Cell Biol.* 125:359–368.

Winckler, B., Ch. Gonzalez Agosti, M. Magendantz, and F. Solomon. 1994. Analysis of a cortical cytoskeletal structure: a role for ezrin-radixin-moesin (ERM proteins) in the marginal band of chicken erythrocytes. *J. Cell Sci.* 107:2523–2534.